SLEEPJ, 2019, 1–9

doi: 10.1093/sleep/zsy235
Advance Access Publication Date: 26 November 2018
Original Article

ORIGINAL ARTICLE

Toward a complete taxonomy of resting state networks across wakefulness and sleep: an assessment of spatially distinct resting state networks using independent component analysis

Evan Houldin[1,2], Zhuo Fang[1,3], Laura B. Ray[1,4], Adrian M. Owen[1,5] and Stuart M. Fogel[1,3–7,*]

[1]Brain and Mind Institute, Western University, London, Canada, [2]Department of Neuroscience, Western University, London, Canada, [3]University of Ottawa Brain and Mind Research Institute, Ottawa, Canada, [4]University of Ottawa Institute for Mental Health Research, Ottawa, Canada, [5]Department of Psychology, Western University, London, Canada, [6]School of Psychology, University of Ottawa, Ottawa, Canada and [7]The Royal's Institute of Mental Health Research, University of Ottawa, Ottawa, Canada

Work Performed: Brain and Mind Institute, Western University, London, Canada

*Corresponding author. Stuart Fogel, School of Psychology, University of Ottawa, Room 3019, Vanier Hall, 136 Jean-Jacques Lussier, University of Ottawa, Ottawa, Ontario, K1N 6N5, Canada. Email: sfogel@uottawa.ca.

Abstract

Resting state network (RSN) functional connectivity (FC) has been investigated under a wealth of different healthy and compromised conditions. Such investigations are often dependent on the defined spatial boundaries and nodes of so-called canonical RSNs, themselves the product of extensive deliberations over distinctions between functional magnetic resonance imaging (fMRI) noise and neural signal, specifically in the context of the healthy waking state. However, a similar unbiased cataloging of noise and networks remains to be done in other states, particularly sleep, a healthy alternate mode of the brain that supports distinct operations from wakefulness, such as dreaming and memory consolidation. The purpose of this study was to explicitly test the hypothesis that there are RSNs unique to sleep. Simultaneous electroencephalography (EEG) and fMRI was used to record brain activity of non-sleep-deprived participants. Independent component analysis was performed on both rapid eye movement (REM; $N = 7$) and non-REM sleep stage fMRI data (non-REM2; $N = 28$, non-REM3; $N = 11$), with the resulting components spatially correlated with the canonical RSNs, for the purpose of identifying spatially distinct RSNs. Surprisingly, all low-correlation components were positively identified as noise, and all high-correlation components comprised the canonical set of RSNs typically observed in wake, indicating that sleep is supported by much the same RSN architecture as wakefulness, despite the unique operations performed during sleep. This further indicates that the implicit assumptions of prior studies, i.e. that the canonical RSNs apply to sleep FC analysis, are valid and have not overlooked sleep-specific RSNs.

Statement of Significance

Resting state network (RSN) functional connectivity (FC) analyses have generated important insights into how brain networks communicate with each other under healthy and pathological conditions. Currently, sleep analyses make use of RSNs defined in wakefulness. However, it remains to be determined whether new RSNs manifest in sleep to support unique sleep-related operations such as dreaming and memory consolidation. Using wakefulness RSNs in sleep analyses could therefore lead to a misinterpretation of distinctions between healthy and pathological brain connectivity in sleep. After searching for new RSNs, this study indicates that sleep is supported by much the same RSN architecture as wakefulness. This clarification is long overdue; improved understanding of sleep brain-connectivity could lead to improved diagnostic tools for pathological sleep conditions.

Key words: EEG; fMRI; sleep; resting state network; REM; non-REM; EEG-fMRI; ICA

Submitted: 23 March, 2018; **Revised:** 1 November, 2018

Introduction

Resting state network (RSN) functional connectivity (FC) has been investigated under a wealth of different conditions including healthy wakefulness [1, 2], sleep states [3], as well as compromised conditions, or altered states of consciousness, such as sedation [4], vegetative state [5], epilepsy [6], Alzheimer's disease [7–9], and schizophrenia [10]. Such investigations often include considerations of both within- and between-RSN FC. However, such considerations are themselves dependent upon the defined spatial boundaries of the RSNs being investigated.

For the most part, these boundaries are taken for granted, as RSNs have now been studied for over two decades, beginning with the identification of the first RSN more than two decades ago, when it was shown that spontaneous activity across bilateral motor networks was strongly correlated [1]. Further studies recognized the existence of other RSNs, including the default mode network (DMN), a set of regions that first came under scrutiny because they collectively reduced their activity during goal-directed tasks [11] and were finally determined to be a unique RSN in their own right when it was acknowledged that they functioned as an interconnected network for supporting "baseline" and internally focused brain activity [12]. The catalogue of reproducible RSNs is now well established, and they are commonly grouped into about 10 canonical networks (see Figure 1A), typically comprising primary sensory networks (e.g. auditory, somatomotor, and up to three visual networks) as well as higher order networks (e.g. DMN, executive control and two independent, lateralized frontoparietal networks). These RSNs noticeably resemble the spatial organization of networks that support discrete cognitive functions [13, 14]. For example, the so-called "auditory" RSN involves bilateral regions in the superior temporal gyrus.

It is the spatial bounds of these canonical RSNs that serve as the basis for between- and within-RSN FC analysis in the aforementioned compromised conditions, states of altered-consciousness and sleep states. Specifically, the regions of interest whose timecourses are used to define RSN FC are based on a priori knowledge of the nodes of RSNs, as they are defined in wakefulness. For example, the well-established finding [3] that FC between anterior and posterior nodes of the DMN is reduced in slow wave sleep makes use of seed-based correlation analysis

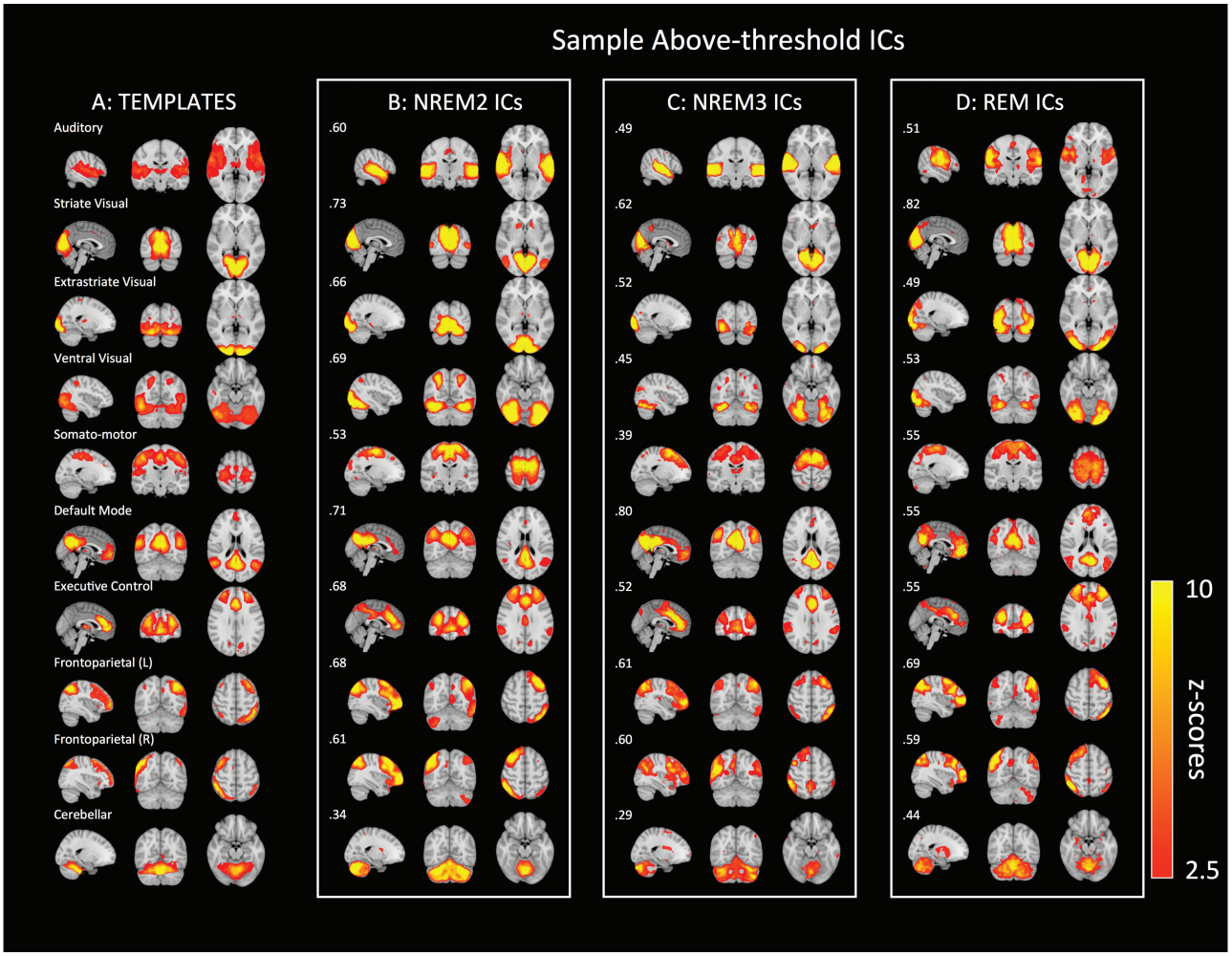

Figure 1. External templates used for spatial comparison and group-level above-threshold independent components (ICs) for each sleep stage. (A) The 10 external templates used in the spatial correlation, with representative sagittal, coronal, and axial slices. (B, C, D) Group-level above-threshold ICs with the highest spatial correlations to each of the 10 external templates, for each sleep stage. Color bars indicate Z statistics based on the estimated standard error of residual noise. Spatial correlation values with respective templates are presented in the upper left corner for each IC. NREM2/3 = non-REM sleep stage 2/3, REM = rapid eye movement sleep stage.

(SCA) wherein the seed of interest is the posterior cingulate cortex (PCC), an important DMN node identified in wakefulness. However, the application of RSNs defined in wakefulness to non-healthy, or sleep-related RSN FC analyses is not fully justified, and the existence of novel RSNs specific to other states has never been explicitly tested or explored. This is the major aim of the current study.

Indeed, given the established association between the canonical RSNs and networks that support cognitive function during healthy wakefulness, it could be expected that noncanonical RSNs would arise to support offline information processing. That said, additional, noncanonical RSNs have yet to be identified in any investigations of non-healthy conditions or healthy sleep states. However, it is possible that such negative findings are at least partly a consequence of biased analysis approaches that make the implicit assumption that the set of RSNs typically found in wakefulness applies to all other conditions. For example, a number of sleep studies have restricted their analysis to RSNs taken from the canonical set (e.g. the DMN [3]) or explicitly looked for RSNs that resemble the canonical set [15], rather than explicitly investigate whether unique RSNs might exist. It therefore remains to be tested whether noncanonical RSNs exist in non-healthy conditions or across healthy sleep-wake states.

Sleep is a particularly salient target for such a test, as it is a healthy alternate mode of the brain, with known functions distinct from the cognitive functions sustained during wakefulness. It is therefore possible that an unbiased search for noncanonical RSNs might yield RSNs associated with these sleep-specific functions. By contrast, compromised conditions or altered states of consciousness are less likely to manifest noncanonical RSNs, given that they do not express new functions; rather the same functions that are expressed in wakefulness become impaired. Unique sleep functions that could manifest unique noncanonical RSNs include memory consolidation (via memory reactivation and replay), involving the striatum, hippocampus, and medial temporal lobe [16–19]; sleep-spindle-related activation that supports reasoning abilities, involving thalamocortical regions and basal ganglia [20]; and rapid eye movement (REM) sleep maintenance, including dream production, involving thalamus and occipital regions [21–23]. Not to mention other putative yet-to-be-discovered functions of sleep.

In addition, sleep can itself be subdivided into at least two further stages, each of which is characterized by unique electroencephalography (EEG) signatures; e.g. REM (demarcated by the presence of eye movements, loss of muscle tone, and desynchronized low-voltage electrophysiological oscillations) and non-REM (NREM) stages. NREM sleep can be further subdivided into NREM stage 1 (NREM1), defined by a loss of posterior alpha band power; stage 2 (NREM2), which sees the appearance of EEG waveforms called sleep spindles and K-complexes; and stage 3 (NREM3) dominated by extensive slow wave delta oscillations [24]. Any of these stages may be accompanied by the manifestation of noncanonical RSNs in relation to these unique forms of neuronal communication that are remarkably distinct from waking brain activity.

The purpose of this study was to explicitly test whether new RSNs exist in sleep by examining all sleep stages for RSNs that do not match the canonical set. It was hypothesized that new RSNs would be identified and that these could be related to sleep-specific neural activation, functions, or mentation specific to sleep.

Methods

Participants

Forty-five participants were recruited for this study. Of these, nine failed to meet the inclusion criteria by not complying with the pre-study sleep/wake schedule, and were thus not included in the study. The remaining 36 were healthy right-handed adults (21 female) 18–34 years of age (M = 23.7, *SD* = 3.6). An a priori statistical power analysis was not performed, which could be considered a limitation; however, the number of participants included is consistent with previous studies investigating RSNs in sleep [3, 15, 25]. All participants were non-shift workers and medication-free, with no history of head injury or seizures; had a normal body mass index (<25); and did not consume excessive caffeine, nicotine, or alcohol. Further, all scored less than 10 on the Beck Depression [26] and the Beck Anxiety [27] Inventories and had no history or signs of sleep disorders, as indicated by the Sleep Disorders Questionnaire [28]. All participants were required to keep a regular sleep–wake cycle (bedtime between 22:00 and 24:00, wake time between 07:00 and 09:00) and to abstain from taking daytime naps at least 7 days prior to, and throughout participation in the study. Adherence with this schedule was monitored using both sleep diaries and wrist actigraphy (Actiwatch 2, Philips Respironics, Andover, MA). All participants met the magnetic resonance imaging (MRI) safety screening criteria. In addition, participants were given a letter of information, provided informed written consent before participation, and were financially compensated for their participation. This research was approved by the Western University Health Sciences Research Ethics Board.

Of the 36 participants who met the study inclusion criteria, data for 34 participants were included in the analysis (see Table 1). One participant withdrew from the study due to discomfort. Another did not sleep during the combined electroencephalography-functional MRI (EEG–fMRI) session but did have wake resting state data. Of the remaining 34 participants (21 female, M = 23.7, *SD* = 3.7), all had wake resting state data, but only 28 had some stage of sleep data above the bare-minimum 3 minute threshold. In addition, not all of the wake resting state data were used, as initially 5 minute wake resting state scans were used, and this was later modified to be 8 minutes, in the interest of maximizing data availability. Thus 29 participants were used in the analysis of the wake data (18 females, M = 23.8, *SD* = 4.0), in order to capitalize on the longer resting state episodes. Of the 28 participants who slept, data from 25 participants were used in the analysis of sleep

Table 1. Minutes of Data Extracted Per Sleep Stage

Measure	Wake	NREM2	NREM3	REM
Mean	7.9	15.9	18.9	9.8
Standard deviation	0.0	10.5	18.9	8.0
Minimum (nonzero)	7.9	6.3	4.0	3.6
Maximum	7.9	44.1	67.3	21.6
N	29/34	25/34	11/34	7/34

REM = rapid eye movement sleep stage, NREM2/3 = non-REM2/3 sleep stages.

stage NREM2 (15 female, M = 24.2, *SD* = 4.0). Of these same 28, 11 participants (6 female, M = 22.5, *SD* = 3.8) had NREM3 data. Finally, of these same 28, 7 participants (3 female, M = 22.1, *SD* = 2.4) had REM data.

Functional data

Wake data set

A total of 36 participants had recorded wake RSN data. Of these, 29 had 7.9 minutes of data, with the remainder having only 5.4 minutes. To maximize the quality of the group independent component analysis (ICA; i.e. by maximizing the number of volumes used in the single-participant data), the wake resting state analysis used the 7.9 minutes datasets from the aforementioned 29 participants, for a total of 230 minutes of data.

Sleep data set

Overall, participants managed to obtain the full spectrum of sleep stages (NREM1, NREM2, NREM3, and REM sleep). On an individual basis, however, the majority of participants maintained sleep in only a few of the stages for a duration long enough to be considered sufficient for ICA analysis. Given the difficulty in obtaining REM sleep in non-sleep-deprived individuals in the MRI scanner environment (e.g. due to noise and participant comfort), only four participants managed to transition through all three sleep-stages of interest (NREM2, NREM3, and REM) for a duration considered sufficient for the ICA analysis. In all cases, sleep scoring identified a pattern in which participants transitioned between sleep stages of variable duration; from less than 20 seconds (the shortest sleep scoring period) to 69.3 minutes (see Table 1 for the distribution of sleep data used in the final set of analyses). As expected, sleep stage NREM1 was mostly insufficient in duration for analysis purposes. Thus, considering the brief and transitional nature of this stage, it was not included in the analyses.

As the group-ICA analysis used in this study requires single-participant inputs of equal length, participant fMRI data for a given sleep stage was segmented into equal length "blocks." Block length was determined by the length of the shortest available single-participant dataset for a given sleep stage (so long as this length exceeded a bare minimum 3 minutes). For example, if 10 participants had NREM3 data, and the participant with the least amount of data had 3 minutes worth, then the available data for the remaining participants was segmented into 3 minute blocks.

Twenty-eight participants were able to sustain a sufficient amount of NREM2 sleep for the ICA analysis, with the shortest duration for a given participant being 4 minutes. In many cases, a single participant had more than one continuous bout of NREM2, such that the full group generated a total of 599 minutes of NREM2 data. Given the abundance of NREM2 data, the datasets for three participants were not included in order to maximize the length of an NREM2 block. Overall, 63 blocks of 6.3 minutes' duration acquired from 25 participants were used, for a total of 396.9 minutes.

In the case of NREM3, 11 participants had data above the minimum 3 minutes' cutoff, for a total of 236.4 minutes of available NREM3 data, with all of these participants having at least 4 minutes of data. Overall, 52 blocks of 4 minutes were used in the ICA analysis of NREM3 data, for a total of 205.9 minutes of data.

Very few EEG–fMRI studies report analysis of REM sleep, and thus knowledge of REM sleep from fMRI studies is limited. Here, 7 participants had REM data above the cutoff of 3 minutes. Overall, 87.7 minutes of 3 minute plus duration data were available from all participants. From this, 19 blocks of 3.6 minutes were extracted for the REM ICA analysis, for a total of 68.4 minutes of data.

Experimental procedure

Each participant underwent a screening/orientation session 1 week prior to the experimental sleep session. The scanning session took place between 21:00 and 24:00, during which time simultaneous EEG–fMRI was recorded while participants slept in the scanner. Unlike the majority of similar past studies, participants were not sleep deprived. The scanning session consisted of a structural scan of 8 minutes, followed by an eyes-closed wake resting state scan. Participants were then informed that they were free to fall asleep in the scanner. This period lasted up to 2.2 hours. To be included in the analysis of the sleep data, participants were required to sleep for a period of at least 5 minutes of uninterrupted NREM sleep during the sleep session; however, in the final analysis no block of less than 3.6 minutes' duration was used. Following the sleep session, participants were allowed to sleep in the nearby sleep laboratory for the remainder of the night.

Polysomnographic recording and analysis

Recording parameters

EEG was recorded using a 64-channel magnetic resonance (MR)-compatible EEG cap (Braincap MR, Easycap, Herrsching, Germany) using two MR-compatible 32-channel amplifiers (Brainamp MR plus, Brain Products GmbH, Gilching, Germany). EEG caps included scalp electrodes referenced to FCz. Two bipolar electrocardiogram (ECG) recordings were taken from V2–V5 and V3–V6 using an MR-compatible 16-channel bipolar amplifier (Brainamp ExG MR, Brain Products GmbH, Gilching, Germany). Using high-chloride abrasive electrode paste (Abralyt 2000 HiCL; Easycap, Herrsching, Germany), electrode-skin impedance was reduced to less than 5 kOhm. In order to reduce movement-related EEG artifacts, participants' heads were immobilized in the MRI head-coil using foam cushions. EEG was digitized at 5000 samples per second with a 500 nV resolution. Data were analog filtered by a band-limited low-pass filter at 500 Hz and a high-pass filter with a time constant of 10 seconds corresponding to a high-pass frequency of 0.0159 Hz. Data were transferred via fiber optic cable to a personal computer where Brain Vision Recorder Software, Version 1.x (Brain Vision, Gilching, Germany) was synchronized to the scanner clock. EEG scanner artifacts were removed in two separate steps: (1) MRI gradient artifacts were removed using an adaptive average template subtraction method [29] implemented in Brain Products Analyzer, and down-sampled to 250 Hz; (2) the r-peaks in the ECG were semiautomatically detected, visually verified, and template subtraction [30] was used to remove ballistocardiographic artifacts time-locked to the R-peak of the QRS complex of the

cardiac rhythm. Finally, EEG was low-pass filtered (60 Hz) and re-referenced to averaged mastoids. Sleep stages were scored in accordance with standard criteria [24] using the "VisEd Marks" toolbox (https://github.com/jadesjardins/vised_marks) for EEGLAB [31].

MRI imaging acquisition and analysis

Recording parameters

Brain images were acquired using a 3.0 T TIM TRIO MRI system (Siemens, Erlangen, Germany) and a 64-channel head coil. A structural T1-weighted MRI image was acquired for all participants using a 3D MPRAGE sequence (TR = 2300 ms, TE = 2.98 ms, TI = 900 ms, FA = 9°, 176 slices, FoV = 256 × 256 mm^2, matrix size = 256 × 256 × 176, voxel size = 1 × 1 × 1 mm^3). Multislice T2*-weighted fMRI images were acquired during the sleep session with a gradient echo-planar sequence using axial slice orientation (TR = 2160 ms, TE = 30 ms, FA = 90°, 40 transverse slices, 3 mm slice thickness, 10% inter-slice gap, FoV = 220 × 220 mm^2, matrix size = 64 × 64 × 40, voxel size = 3.44 × 3.44 × 3 mm^3). In order to obtain EEG with time-stable artifacts, which aligned to the timing of the EEG recordings, the MR scan repetition time was set to 2160 ms, such that it matched a common multiple of the EEG sample time (0.2 ms), the product of the scanner clock precision (0.1 μs), and the number of slices (40) used [32].

Functional data classification and block parcellation

All sleep session functional volumes were scored according to standard sleep-stage scoring criteria [24] by an expert, registered polysomnographic technologist. To be included in the fMRI analysis, the EEG had to be visibly movement artifact-free. Volumes were classified as wake, NREM1, NREM2, NREM3, or REM. Notably, wake data used in the analysis were taken from the wake resting state session only, despite segments of wake being present in the sleep session data. Following scoring, each segment of sleep-stage volumes was parcellated into equal-size blocks, whose length was specific to each given sleep stage.

Preprocessing

Blocks were individually preprocessed using the Oxford Centre for Functional Magnetic Resonance Imaging of the Brain Software Library (FMRIB, Oxford, United Kingdom; FSL version 5.09 [33]). Specifically, functional volumes within each block were realigned using FSL's MCFLIRT tool [34], which performs rigid body transformations. Non-brain voxels were also extracted using FSL's BET tool [35]. Volumes were then spatially smoothed using a Gaussian kernel of 5 mm full-width at half-maximum (FWHM) and high-pass temporal filter (Gaussian-weighted least-squares straight line fitting, FWHM = 2000 s). Functional volumes were then registered to the MNI152 standard space (McConnell Brain Imaging Centre, Montreal Neurological Institute) using 12 degree-of-freedom affine registration. Finally, each block was individually cleaned of nonneuronal artifacts (e.g. cardiac pulsation, motion related, white matter [WM]) using the FIX plug-in for the FSL package [36, 37], an automatic noise detection and removal algorithm. Prior to using FIX, FSL's MELODIC tool [38] was used to generate a set of independent components (ICs) for each block. MELODIC prewhitens and variance normalizes all time series prior to applying probabilistic ICA, which outputs a set of spatial maps converted into Z statistic maps based on estimated standard error of residual noise. MELODIC's default dimensionality estimation function automatically estimates the number of ICs by performing a Bayesian analysis. FIX assessed each of these ICs as noise or signal, after identifying more than 180 distinct spatial and temporal features for each IC and feeding these into a multilevel classifier. Temporal features associated with nonneuronal ICs include sudden changes in time series' amplitude, frequency-domain power at high frequencies, and correlation of the time series with WM or cerebrospinal fluid (CSF) extracted time series. Spatial features include having a large number of small clusters and high overlap with brain boundaries or with WM/ventricles/CSF areas. FIX classification performance has been evaluated to have an average true negative rate (noise correctly classified as such) of 98.9% [36]. ICs classified as noise were then subtracted from the ICA mixing matrix and a new set of "clean" functional volumes was generated.

Group-level analysis

Group spatial ICA (with a model order of 30 components) was performed with MELODIC on all available blocks for a given sleep stage in order to maximize the available data for deriving group-level maps. The resulting 30 ICs (per sleep stage) were then individually compared with 10 canonical spatial templates derived from a separate wake RSN study [14] (see Figure 1A) using spatial correlation (FSL utility; fslcc). In order to be consistent with current approaches, a liberal spatial correlation threshold of $r > 0.2$ was selected (for comparison, Tong *et al.* [39] and Reineberg *et al.* [40] used similar cutoffs of $r > 0.25$ and $r > 0.21$, respectively) to help classify ICs as either resembling the canonical set or being a potentially new RSN for further inspection (See Supplementary Figure S3 in the Supplemental Material for the distribution of available correlation values in this study). However, both above- and below-threshold ICs were also (visually) examined carefully for spatial differentiation from the canonical set. It is important to emphasize here that the use of a specific spatial correlation threshold (statistically based, or otherwise) will always be arbitrary, in the case of classifying ICs as RSNs. This is because RSN classification must always take into account other IC features, such as frequency–power. That said, a threshold of around $r > 0.2$ seems to work as a useful heuristic for early IC screening. Clearly identifiable noise-related below-threshold components were then screened by hand, in accordance with the general guidelines in Griffanti *et al.* [41] and Kelly *et al.* [42]. Note that it is impossible to completely separate noise from networks in fMRI data, at either the single-participant or group level; therefore, noise ICs would be expected at the group level despite cleaning at the single-participant level (more specifically, timecourse patterns associated with noise can be too infrequent for ICA to detect at the single-participant level, yet, importantly, they can repeat sufficiently across multiple participants, so that they manifest as statistically independent and can therefore be reliably detected at the group level). Briefly, in the screening procedure, IC spatial features were examined for overlap with non-gray matter areas such as those comprising WM or CSF and IC frequency–power spectra

were examined for power distribution across all frequencies, or power concentration in high frequencies. The intention was to follow-up this screening with a more sophisticated fingerprint analysis tool [43], as well as a FC analysis between candidate components and the canonical RSNs; however, the lack of remaining components following this screening procedure rendered such steps unnecessary.

Finally, we conducted a follow-up analysis in which we repeated the group-level ICA analysis described earlier, using a dataset consisting of all of the sleep stages combined together (note: in this analysis, the blocks were cut to the same length across sleep stages; i.e. to 129 volumes). This was done in an attempt to determine whether the ICA might extract new spatial patterns that would otherwise be missed in an analysis of individual sleep stage data.

Results

ICA analysis and template comparison

Non-noise group-level above-threshold ICs largely matched the RSNs from the external dataset [14], with low correlation components comprising constituent regions of a given canonical RSN rather than being located in a different spatial region entirely (see Figure 1 for sample images).

Sample below-threshold ICs are shown in Figure 2, along with their frequency–power spectra. All below-threshold ICs had time course properties that allowed them to be positively identified as nonneuronal artifacts, in accordance with standard identification procedures [41, 42]. For example, the first IC in Figure 2A overlaps significantly with WM regions and the second IC overlaps with CSF-containing regions and also has power distributed across all frequencies (i.e. it is not restricted to low frequencies as is typical of RSNs). As such, contrary to our predictions, none could be said to represent spatially unique RSNs differentiable from canonical RSNs in any sleep stage of interest.

The follow-up analysis (in which the group ICA was performed on a dataset composed of all the sleep-stage data combined together) yielded similar results; i.e. above-threshold ICs largely matched the RSNs from the external dataset and below-threshold ICs were positively identified as nonneuronal artifacts (see Figure 3 for sample images).

Finally, for reference, color-coded correlation values for all 30 group-level ICs for all stages (including the combined-stages dataset) are presented in the Supplementary Material (see Supplementary Figures S1 and S2), with their best-matched external templates indicated.

Discussion

This is the first study to use combined EEG and fMRI to examine all sleep stages with the explicit purpose of identifying noncanonical sleep-specific RSNs. It was hypothesized that some new RSNs would be discovered and that these could be related to aspects of mentation specific to sleep, much as waking cognitive functions are related to the canonical RSNs. Surprisingly, no new sleep-specific RSNs were found in any sleep stage, despite a directed search using a uniquely rich dataset, as all below-threshold ICs were carefully inspected and positively identified as nonneuronal artifacts. These results strongly suggest that there are no sleep-specific RSNs. Rather, the canonical RSNs that seemingly support waking mentation also support (or at the very least, co-occur with) sleep-specific functions and thus, the repertoire of canonical RSNs present in wake comprises the full set across sleep-wake states.

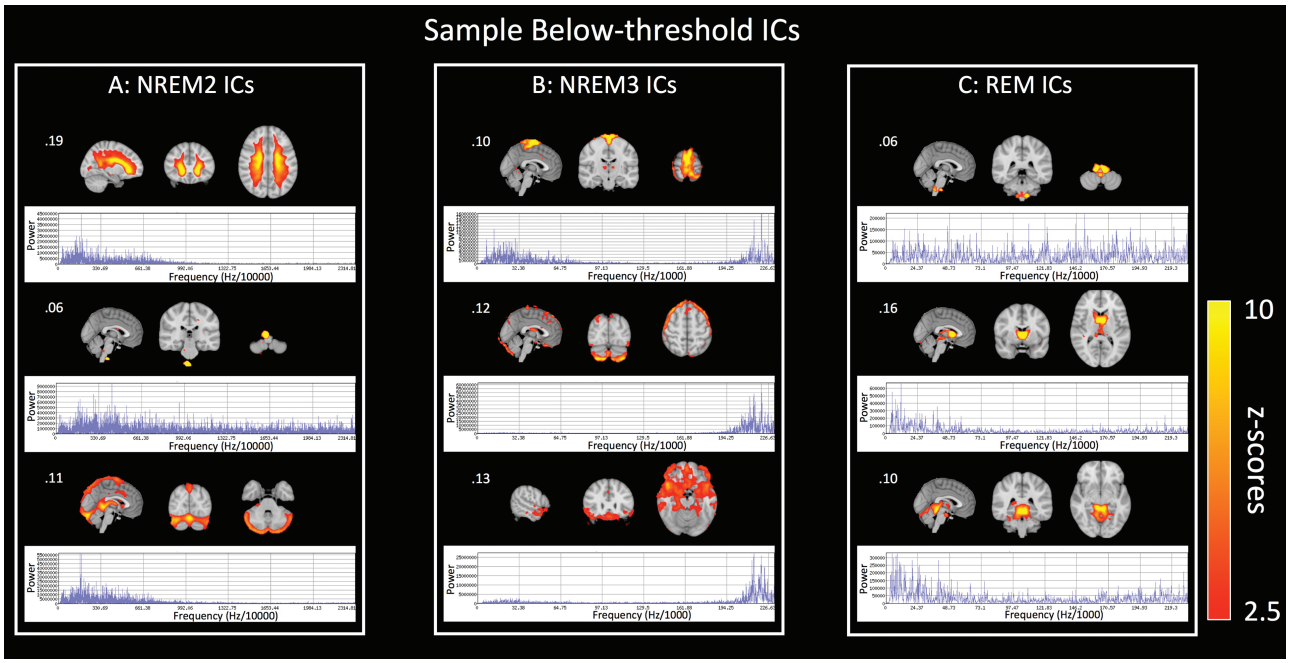

Figure 2. Sample below-threshold independent components (ICs) in each sleep stage. (A, B, C) A selection of below-threshold group-level ICs, for each sleep stage (representative sagittal, coronal, and axial slices shown). Color bars indicate Z statistics based on the estimated standard error of residual noise. Frequency–power spectra are shown immediately below each IC. Highest template-correlation value is indicated in top left corner for each IC. NREM 2/3 = non-REM sleep stage 2/3, REM = rapid eye movement sleep stage.

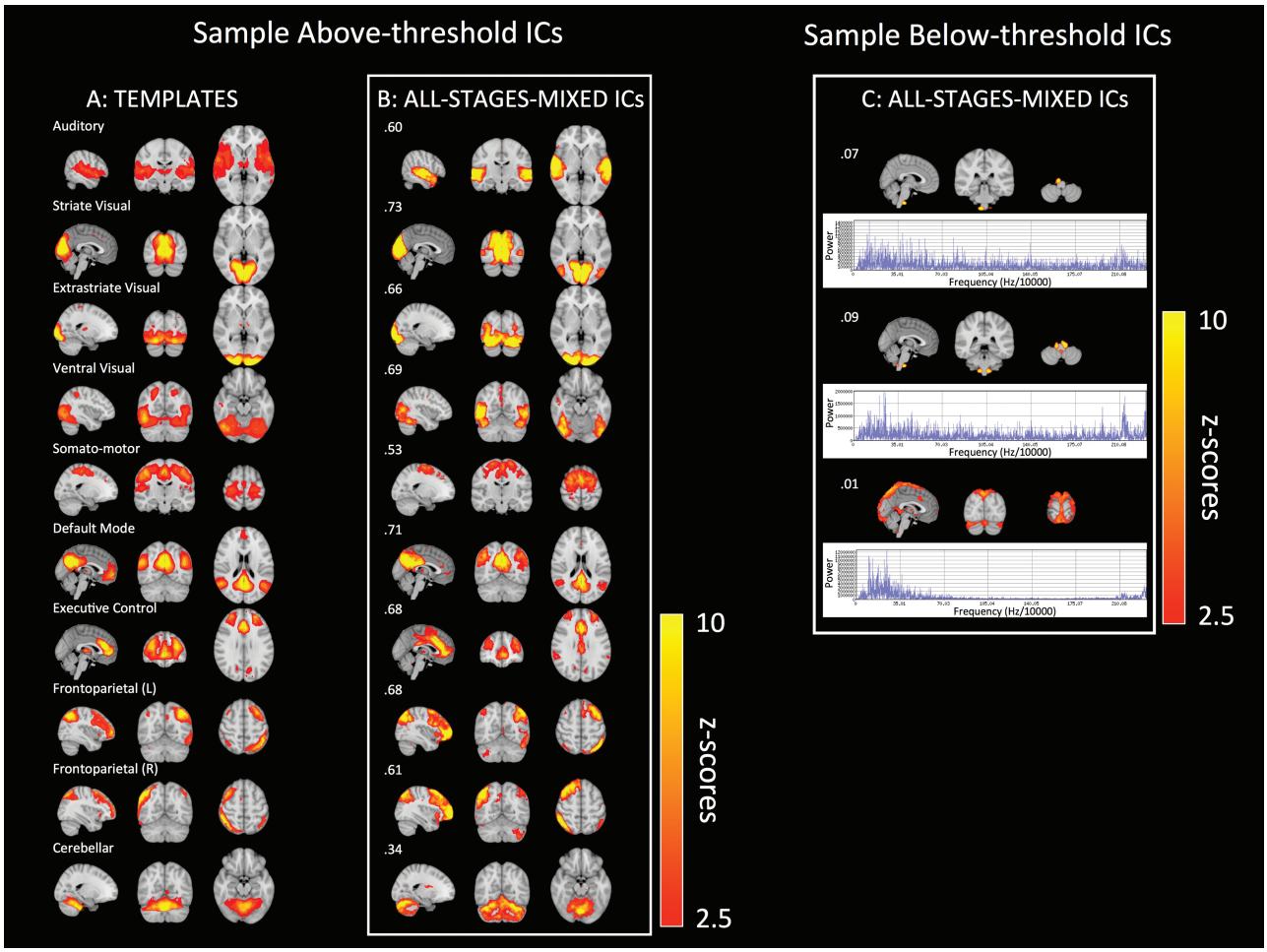

Figure 3. External templates used for spatial comparison and group-level above-threshold independent components (ICs), with sample below-threshold ICs for a dataset composed of all sleep stages combined. (A) The 10 external templates used in the spatial correlation, with representative sagittal, coronal, and axial slices. (B) Group-level above-threshold ICs with the highest spatial correlations to each of the 10 external templates, for a dataset composed of all sleep stage data combined together. Color bars indicate Z statistics based on the estimated standard error of residual noise. Spatial correlation values with respective templates are presented in the upper left corner for each IC. (C) A selection of below-threshold group-level ICs (representative, sagittal, coronal, and axial slices shown). Color bars indicate Z statistics based on the estimated standard error of residual noise. Frequency–power spectra are shown immediately below each IC. Highest template-correlation value is indicated in top left corner for each IC.

Moreover, the results of previous RSN FC studies that made use of RSN nodes defined by wakefulness studies can now be confirmed to stand on more solid ground, and appear to have not inadvertently overlooked sleep-specific RSNs. Importantly, these findings suggest that the unique functions (e.g. offline memory consolidation), cognitive processes (e.g. dreaming), electrophysiological features and forms of communication (e.g. spindles, k-complexes, slow waves), which characterize sleep stages (e.g. NREM1, 2, 3, REM), surprisingly, do not manifest or require unique sleep-specific RSNs.

There are a number of methodological limitations that could explain this result. In particular, the quality of a search for a new RSN can only be measured against two definitions; what currently constitutes an RSN and what might constitute an RSN unique from what is currently defined as an RSN. Given that the functional role of RSNs is presently speculative, such definitions must be delimited by a collection of spatial and temporal properties, the most important of which are those that would rule out a potential RSN from being a known source of nonneuronal blood oxygen level dependent artifacts. If this study has failed to recognize the existence of a "sleep-RSN," then this failure likely rests on the assumptions made about the spatial and temporal properties most commonly used to identify RSNs.

As far as spatial properties are concerned, it is reasonable to question whether the spatial templates in Smith *et al.* [14], used to rule out group-level ICs as being new RSNs, were a fair representation of canonical RSNs. These 10 templates were themselves generated from a 20 model-order ICA decomposition, and hence their spatial bounds are specific to this decomposition. A comparison of ICs from this study against external templates generated from a different model order would surely yield different results. On the other hand, although the correlation values would have changed, visual inspection of components would indicate that the same networks were being represented, albeit in a reduced or more elaborated form. Nevertheless, Ray *et al.* [44] performed an assessment of ICA dimensionalities ranging in size from 20 to 200 and found that a dimensionality of around 20 is appropriate for examining RSNs at the scale of the 10 canonical RSNs. This same rationale

applies to the use of a 30 model-order decomposition for the data in this study.

An additional challenge involves the use of an automatic ICA de-noising algorithm to clean the individual blocks. This algorithm makes use of spatial and temporal property weightings that are biased toward what current RSN experts deem to be a nonneuronal artifact in wake resting state data. It is entirely possible that RSNs in sleep exhibit different temporal and spatial properties from their waking counterparts, e.g. power at oscillatory high-frequency that would cause them to be rejected as noise by an expert (or automated software tuned to the judgment of an expert). Further, without knowing the true functional role and neurological mechanisms of RSNs, there will always be some uncertainty in defining either RSNs or nonneuronal artifacts outside of their normal milieu (i.e. waking conditions).

Such concerns can be mitigated when considering the general robustness of the essential spatial configuration and temporal properties of RSNs under compromised or pathological conditions. There is therefore some measure of confidence that an RSN will have recognizable properties under healthy physiological conditions alternate to wake.

A more contentious issue might be the resting state lengths used in the analysis. The NREM3 and REM analyses made use of 4 and 3.6 minutes' duration blocks, respectively. Resting state analyses typically utilize 5–7 minutes of data, and it has been suggested that a 12–16 minutes resting state scan time is ideal [45]. However, given the difficulty in acquiring NREM3 and REM fMRI data, the short block lengths were considered reasonable. For comparison, a similar EEG–fMRI sleep study by Chow *et al.* [46] (prior to the current study, this was the largest available EEG–fMRI dataset available for REM) acquired 32.4 minutes of REM data from 4 participants out of an initial pool of 18, all of whom were sleep deprived for 44 hours prior to the study; this study acquired 75.2 minutes of REM data from 7 participants out of an initial pool of 35, none of whom were sleep deprived. The inadequacy of these datasets would appear to be unlikely, however, given the identification of robust canonical RSNs in both of these stages; however, Type II error (i.e. concluding that new RSNs are not present in sleep) is still a possibility.

Further, it should be noted that the ICA results are potentially biased by the extra number of blocks drawn from single-participant data with more volumes available for a given sleep stage. This was considered an acceptable risk, in order to maximize the data available for the sleep ICA analysis. In order to test whether this was possibly problematic, we repeated the analysis using only a single block for each participant with data available for a given stage, and were able to confirm the same pattern of results using this alternative approach.

Finally, it is worth pointing out that the well-established finding that the DMN breaks up into anterior and posterior nodes during slow wave sleep [3] is not contradicted by the present results, which indicate that the DMN can be detected across all sleep stages. This apparent discrepancy likely emerges from the different aims and approaches used in previous studies, which employed SCA. SCA looks at whole-brain correlations with the average timecourse within a "seed" region (e.g. the PCC). By contrast, this study employed ICA, which finds statistically ICs by maximizing the non-Gaussianity of a dataset. It is therefore consistent for a "complete" DMN (i.e. comprising anterior and posterior components), detected as a distinct component using ICA, to coexist with a less cohesive DMN, as identified using SCA methodology. Hence, the present results can be considered to be complementary with previous studies, given the differing approaches; our results show that the DMN is present in all sleep stages, but previous studies show that cohesiveness of the DMN varies as a function of sleep depth. Although beyond the scope of this study, future studies should consider other approaches, importantly, a comprehensive analysis of RSN FC differences across wakefulness and all sleep stages.

In conclusion, although canonical RSNs have been identified in sleep in a number of prior studies, these studies were not explicitly looking for RSNs beyond the waking set, and as a consequence would not have included these networks in their investigation, nor were they comprehensive (with REM often excluded; understandable given the difficulty of acquiring REM fMRI data). Consequently, this is the first study that explicitly tested whether the full inventory of RSNs is known across sleep/wake states and represents a further step in the direction of defining a complete taxonomy of RSNs.

Supplementary Material

Supplementary material is available at *SLEEP*online.

Funding

This research was funded by a Canada Excellence Research Chair (CERC) grant to author AMO.
Conflict of interest statement. None declared.

References

1. Biswal B, *et al.* Functional connectivity in the motor cortex of resting human brain using echo-planar MRI. *Magn Reson Med*. 1995;**34**(4):537–541.
2. Smith SM, *et al.*; WU-Minn HCP Consortium. Resting-state fMRI in the Human Connectome Project. *Neuroimage*. 2013;**80**:144–168.
3. Horovitz SG, *et al.* Decoupling of the brain's default mode network during deep sleep. *Proc Natl Acad Sci U S A*. 2009;**106**(27):11376–11381.
4. Boveroux P, *et al.* Breakdown of within- and between-network resting state functional magnetic resonance imaging connectivity during propofol-induced loss of consciousness. *Anesthesiology*. 2010;**113**(5):1038–1053.
5. Boly M, *et al.* Functional connectivity in the default network during resting state is preserved in a vegetative but not in a brain dead patient. *Hum Brain Mapp*. 2009;**30**(8):2393–2400.
6. Centeno M, *et al.* Network connectivity in epilepsy: resting state fMRI and EEG-fMRI contributions. *Front Neurol*. 2014;**5**:93.
7. Vemuri P, *et al.* Resting state functional MRI in Alzheimer's disease. *Alzheimers Res Ther*. 2012;**4**(1):2.
8. Sorg C, *et al.* Selective changes of resting-state networks in individuals at risk for Alzheimer's disease. *Proc Natl Acad Sci U S A*. 2007;**104**(47):18760–18765.
9. Wang K, *et al.* Discriminative analysis of early Alzheimer's disease based on two intrinsically anti-correlated networks with resting-state fMRI. *Med Image Comput Comput Assist Interv*. 2006;**9**(Pt 2):340–347.

10. Yu Q, *et al*. Brain connectivity networks in schizophrenia underlying resting state functional magnetic resonance imaging. *Curr Top Med Chem*. 2012;**12**(21):2415–2425. doi:10.2174/156802612805289890.
11. Shulman GL, *et al*. Common blood flow changes across visual tasks: i. increases in subcortical structures and cerebellum but not in nonvisual cortex. *J Cogn Neurosci*. 1997;**9**(5):624–647.
12. Raichle ME, *et al*. A default mode of brain function. *Proc Natl Acad Sci U S A*. 2001;**98**(2):676–682.
13. Damoiseaux JS, *et al*. Consistent resting-state networks across healthy subjects. *Proc Natl Acad Sci U S A*. 2006;**103**(37):13848–13853.
14. Smith SM, *et al*. Correspondence of the brain's functional architecture during activation and rest. *Proc Natl Acad Sci U S A*. 2009;**106**(31):13040–13045.
15. Tagliazucchi E, *et al*. Breakdown of long-range temporal dependence in default mode and attention networks during deep sleep. *Proc Natl Acad Sci U S A*. 2013;**110**(38):15419–15424.
16. Stickgold R. Sleep-dependent memory consolidation. *Nature*. 2005;**437**(7063):1272–1278.
17. Marshall L, *et al*. The contribution of sleep to hippocampus-dependent memory consolidation. *Trends Cogn Sci*. 2007;**11**(10):442–450.
18. Rattenborg NC, *et al*. Hippocampal memory consolidation during sleep: a comparison of mammals and birds. *Biol Rev Camb Philos Soc*. 2011;**86**(3):658–691.
19. Fogel S, *et al*. Reactivation or transformation? Motor memory consolidation associated with cerebral activation time-locked to sleep spindles. *PLoS One*. 2017;**12**(4):e0174755.
20. Fang Z, *et al*. Neural Correlates of human cognitive abilities during sleep. *BioRxiv* April 2017:130500. doi:10.1101/130500.
21. Nelson JP, *et al*. REM sleep burst neurons, PGO waves, and eye movement information. *J Neurophysiol*. 1983;**50**(4):784–797.
22. Hobson JA, *et al*. Dreaming and the brain: toward a cognitive neuroscience of conscious states. *Behav Brain Sci*. 2000;**23**(6):793-842. doi:10.1017/S0140525X00003976.
23. Klemm WR. Why does rem sleep occur? A wake-up hypothesis. *Front Syst Neurosci*. 2011;**5**:73.
24. Iber C, *et al*. The AASM Manual for the Scoring of Sleep and Associated Events: Rules, Terminology and Technical Specifications; 2007. Westchester, IL: American Academy of Sleep Medecine. doi:10.1002/ejoc.201200111
25. Larson-Prior LJ, *et al*. Cortical network functional connectivity in the descent to sleep. *Proc Natl Acad Sci U S A*. 2009;**106**(11):4489–4494.
26. Beck AT, *et al*. Manual for the Beck Depression Inventory-II. 1996. San Antonio, TX: Psychological.
27. Beck AT, *et al*. An inventory for measuring clinical anxiety: psychometric properties. *J Consult Clin Psychol*. 1988;**56**(6):893–897. doi:10.1037/0022-006X.56.6.893.
28. Douglass AB, *et al*. The sleep disorders questionnaire. I: creation and multivariate structure of SDQ. *Sleep*. 1994;**17**(2):160–167. doi:10.1093/sleep/17.2.160.
29. Allen PJ, *et al*. A method for removing imaging artifact from continuous EEG recorded during functional MRI. *Neuroimage*. 2000;**12**(2):230–239.
30. Allen PJ, *et al*. Identification of EEG events in the MR scanner: the problem of pulse artifact and a method for its subtraction. *Neuroimage*. 1998;**8**(3):229–239.
31. Delorme A, *et al*. EEGLAB: an open source toolbox for analysis of single-trial EEG dynamics including independent component analysis. *J Neurosci Methods*. 2004;**134**(1):9–21.
32. Mulert C, *et al*., ed. *EEG-fMRI; Physiological Basis, Technique, and Applications*. Switzerland: Springer Nature; 2009;538. doi:10.1007/978-3-540-87919-0.
33. Smith SM, *et al*. Advances in functional and structural MR image analysis and implementation as FSL. *NeuroImage*. 2004;**23**(Suppl 1):S208–S219. doi:10.1016/j.neuroimage.2004.07.051.
34. Jenkinson M, *et al*. Improved optimization for the robust and accurate linear registration and motion correction of brain images. *Neuroimage*. 2002;**17**(2):825–841.
35. Smith SM. Fast robust automated brain extraction. *Hum Brain Mapp*. 2002;**17**(3):143–155.
36. Salimi-Khorshidi G, *et al*. Automatic denoising of functional MRI data: combining independent component analysis and hierarchical fusion of classifiers. *Neuroimage*. 2014;**90**:449–468.
37. Griffanti L, *et al*. ICA-based artefact removal and accelerated fMRI acquisition for improved resting state network imaging. *Neuroimage*. 2014;**95**:232–247.
38. Beckmann CF, *et al*. Probabilistic independent component analysis for functional magnetic resonance imaging. *IEEE Trans Med Imaging*. 2004;**23**(2):137–152.
39. Tong Y, *et al*. Can apparent resting state connectivity arise from systemic fluctuations? *Front Hum Neurosci*. 2015;**9**:285. doi:10.3389/fnhum.2015.00285.
40. Reineberg AE, *et al*. Resting-state networks predict individual differences in common and specific aspects of executive function. *Neuroimage*. 2015;**104**:69–78.
41. Griffanti L, *et al*. Hand classification of fMRI ICA noise components. *Neuroimage*. 2017;**154**:188–205.
42. Kelly RE Jr, *et al*. Visual inspection of independent components: defining a procedure for artifact removal from fMRI data. *J Neurosci Methods*. 2010;**189**(2):233–245.
43. De Martino F, *et al*. Classification of fMRI independent components using IC-fingerprints and support vector machine classifiers. *Neuroimage*. 2007;**34**(1):177–194.
44. Ray KL, *et al*. ICA model order selection of task co-activation networks. *Front Neurosci*. 2013;**7**:237.
45. Birn RM, *et al*. The effect of scan length on the reliability of resting-state fMRI connectivity estimates. *Neuroimage*. 2013;**83**:550–558.
46. Chow HM, *et al*. Rhythmic alternating patterns of brain activity distinguish rapid eye movement sleep from other states of consciousness. *Proc Natl Acad Sci U S A*. 2013;**110**(25):10300–10305.